JOURNAL OF CHEMICAL & ENGINEERING DATA

Article

pubs.acs.org/jced

Thermodynamic Properties and Crystal Structures of the Adductive 2,6-Naphthalenedicarboxylic Acid Crystallization with *N*,*N*-Dimethyl Acetamide and *N*-Methyl Pyrrolidone

Bianhua Wu, Youwei Cheng,* and Xi Li

Department of Chemical and Biological Engineering, Zhejiang University, Hangzhou 310027, People's Republic of China

ABSTRACT: The crystal structures and thermodynamic properties of NDA-DMAC and NDA-NMP adduct crystals, the solubilities of 2,6-naphthalenedicarboxylic acid (NDA) in *N*,*N*-dimethyl acetamide (DMAC) and *N*-methyl pyrrolidone (NMP) over a temperature range from (293.2 to 373.2) K were studied in this paper. The results show that: (1) The asymmetric units of NDA-DMAC and NDA-NMP adduct crystals both contain one half molecule of NDA and one molecule of the solvent which are linked mainly by hydrogen bonds. (2) The thermal stabilities of the two adducts are both poor, and the initial dissociation temperature of NDA-DMAC and NDA-NMP adducts are about 306.29 K and 322.75 K, respectively. (3) The solubilities of NDA in DMAC and NMP solvents at (293.2 to 373.2) K both increase with the rise of experimental temperature. Below the dissociation temperature, the equilibrium solid phase is the adduct crystal with the adduct solvent. Otherwise, the equilibrium solid phase is the pure NDA solid with the adduct crystal dissociating. The solubility data are correlated by the Buchowski equation or the nonrandom two-liquid (NRTL) activity coefficient model.

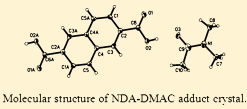

Molecular structure of NDA-DMAC adduct crystal.

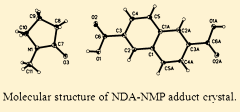

Molecular structure of NDA-NMP adduct crystal.

INTRODUCTION

2,6-Naphthalenedicarboxylic acid (NDA) is an important monomer for the production of polyester, polyurethane, and liquid crystal polyester (LCP). The most popular application is polymerization with ethylene glycol to produce poly(ethylene 2,6-naphthalenedicarboxylate) (PEN). With a super gas barrier property, great heat-resistant quality, mechanical property, and chemical stability relative to other polyester materials, PEN has been widely used to manufacture high performance bottles, films, fibers, and other shaped articles. Although there is a huge demand of PEN every year all over the world, the PEN output is subject to the inefficient production of 2,6-NDA.[1]

NDA is typically produced by the liquid-phase, metal-catalyzed oxidation of dialkylnaphthalene.[2,3] The crude NDA product always has residual catalyst metals and organic impurities formed during the oxidation process, including trimellitic acid, bromo-2,6-NDA, 2-formyl-6-naphthoic acid, 2-naphthoic acid, and so on. These impurities have an adverse effect on the substantial synthesis of polymers.[2,4] They can restrict the polymerization speed and molecular weight of the polymer and affect the performance and color of the polymer product badly. So removing the impurities to a lower level acceptable for polymerization is essential. However, it is difficult to purify NDA through conventional methods, such as recrystallization, rectification, and sublimation, due to its high melting point, its low solubility in most solvents, and its similarities in physical and chemical properties with impurities.

The purification method of NDA has attracted great interest and been extensively studied. Rusins et al.[5] has developed a method where, after reacting with a substantial excess of acetic anhydride, the crude NDA solution is recrystallized and then hydrolyzed to obtain highly purified NDA. Iwane et al.[6] has suggested solving the crude NDA in an organic solvent, treating the solution with active carbon, and then recrystallizing the purified NDA. Other arts, such as catalytic hydrogenation, esterification−hydrolyzation, and chlorization, have been conducted, too.[2,4,7] Unfortunately, all of these methods seem to be unsatisfactory and too complicated and high-cost to be improved well enough for industrialization.

In this paper, a new separation and purification method, adductive crystallization, was applied to purify the crude NDA.[8] Adductive crystallization is a kind of operation that, with an extraneous agent added to the feed, produces a crystalline solid phase which is the adduct of the feed and the agent gradually. Then the adduct crystal can be separated from the mother liquid by filtering.[9−11] The easy decomposition property of the adduct is preferable. Thus, the highly purified solute can be obtained, and the solvent can be recycled easily. The adductive crystallization method has been reported to separate and purify terephthalic acid in previous works.[10−12]

In view of the properties of NDA, amides were considered to be promising adduct solvents in this study. As adduct solvents, amides such as *N*,*N*-dimethyl acetamide (DMAC), *N*-methyl pyrrolidone (NMP), *N*,*N*-dimethyl formamide (DMF), *N*,*N*-dimethyl propionamide (DMP), *N*,*N*-diethyl acetamide (DEA), and *N*,*N*-diethyl propionamide (DEP), were studied in the adductive crystallization process of NDA. At room temperature, about 0.1 g of crude NDA product was placed in 1 mL solvent in a sealed tube. After 72 h, the tubes without any crystal appearing were transferred to a freezer kept at 253.15 K, with an expectation for the crystal to appear at a lower temperature. The temperature, 253.15 K, was determined by the melting

Received: September 14, 2011
Accepted: December 22, 2011
Published: January 18, 2012

points of the solvents. It was found that DMAC and NMP could give visible NDA-DMAC and NDA-NMP adduct crystals at room temperature, while other amides could not result in any adducts even at 253.15 K. So DMAC and NMP were chosen as the proper adduct solvents here.

Since the adductive crystallization is a meaningful method for purifying NDA, the basic data related to these two adductive crystallization processes were studied. The structures and thermodynamic properties of NDA-DMAC and NDA-NMP adduct crystals were provided by X-ray diffraction (XRD) and differential scanning calorimetry (DSC) analysis, respectively. The solubility data of NDA in DMAC and NMP solvents were presented and correlated by the Buchowski equation or the nonrandom two-liquid (NRTL) activity coefficient model. All of these data were the foundation of the substantial study about the separation and purification process of NDA by the adductive crystallization method.

EXPERIMENTAL PROCEDURE

Chemicals. The crude NDA product with a mass fraction purity greater than 88 % was produced by the 2,6-diisopropylnaphthalene (2,6-DIPN) oxidation method in our own laboratory. The standard NDA reagent (mass fraction purity > 98 %) was purchased from Tokyo Kasei Kogyo Co., Ltd. DMAC, NMP, DMF, DMP, DEA, DEP, and absolute methanol of analytical grade were supplied by Tianjin BODI Chemical Reagent Co. (mass fraction purity > 99.5 %). High-performance liquid chromatography (HPLC) grade methanol and acetonitrile were obtained from the USA Tedia Company, Inc. (mass fraction purity > 99.9 %). Dimethyl sulfoxide (DMSO) and demineralized water were produced by Hangzhou Chemical Reagent Co. All reagents could be used as received without any pretreatments.

Solubilities of NDA in DMAC and NMP. A sample of 7 g of standard NDA reagent was placed in 50 mL of solvent in a jacketed equilibrium glass bottle which was sealed by a rubber stopper to prevent the evaporation of the solvent and was put in a thermostatic oil bath. A magnetic bar was put in the bottle for stirring. A thermometer pierced the stopper until the sampling position to control the sampling temperature precisely. The uncertainty of the experimental temperature was estimated to ± 0.5 K.

After determining the equilibrium time, the experiments measuring the solubilities of NDA in DMAC and NMP were performed at temperatures ranging from (293.2 to 373.2) K. Continuous stirring was carried out for enough time, and then 24 h of standing time was needed to verify the sufficient clearness of the liquid phase. Afterward, the saturated NDA solution was sampled for analysis every 3 h until the results were reproducible to within ± 1 %. In each sampling process, about 0.1 mL of the saturated NDA solution, namely, the clear upper portion of the solution was transferred by a 0.25 mL syringe into a 25 mL volumetric flask. Some emphasis should be placed here. First, the syringe and the volumetric flask used for sampling were preheated at a temperature 20 K higher than the experimental temperature to avoid the crystallization of the solute during the sampling process. Second, the sample was taken as fast as possible, and the volumetric flask was shut up immediately. After cooling down to the room temperature, the sample was weighed. With the mass of the volumetric flask subtracted, the mass of the sample solution was obtained. Then the partly crystallized sample solution was dissolved by DMSO and diluted quantitatively with absolute methanol to 25 mL for analysis.

Analytical Methods. The precise structures of NDA-DMAC and NDA-NMP adduct crystals were determined by XRD, using an Oxford Diffraction Xcalibur (Atlas Gemini ultra) diffractometer. The crystal was fixed on the top of a glass fiber, and the related data were collected by the diffractometer using a Mo Kα ray (λ = 0.71073) made from graphite monochromatization and a ω-2θ scanning mode with 2θ ranging from 2.75° to 29.28° for the NDA-DMAC adduct and from 3.09° to 29.17° for the NDA-NMP adduct.[13]

The thermal stabilities of NDA-DMAC and NDA-NMP adduct crystals were analyzed by the differential scanning calorimeter (DSC), Q200 DSC, with nitrogen protection. The samples were sealed in aluminum plates and heated at the heating rate of 10.00 K·min^{-1} from (313.15 to 373.15) K, isothermal for 3.00 min, then cooled at 10.00 K·min^{-1} to −183.15 K, isothermal for 3.00 min, then heated to 373.15 K again at 10.00 K·min^{-1}, and isothermal for 2.00 min; then the cooling and heating cycle was repeated to verify the reversibility of the dissociation and generation process of the adduct crystals and the repeatability of the experimental data.

The composition of the saturated NDA solution was determined by the HPLC analysis using the external reference method which was carried out by an Agilent 1100. A Diamonsil C18 (250 × 4.6 mm, Φ 5 μm) chromatographic column and a DAD UV detector (254 nm) were used at 303.15 K here. The mobile phase consisted of three eluents: methanol, water, and acetonitrile. The adopted three-component gradient elution program was listed in Table 1, and the change of the composition was linear with time.

Table 1. Three-Component Gradient Elution Program in HPLC

time/min	mass fraction of methanol/%	mass fraction of water/%	mass fraction of acetonitrile/%
0	5	75	20
3	10	55	35
9	10	15	75
12	0	0	100

RESULTS AND DISCUSSION

Crystal Structures of the Adduct Crystals. According to the XRD results, the crystal structures of the adducts were worked out by the direct method using SHELX-97 procedures.[14] The main structure information of the adduct crystals NDA-DMAC and NDA-NMP is listed in Table 2, and the structures are shown in Figures 1 and 2. The asymmetric units of the two crystals both contain one half molecule of NDA and one molecule of the solvent, and they are linked by O−H···O hydrogen bonds and C−H···O interactions.[11]

Thermodynamic Properties of the Adduct Crystals. The curves of the two cooling−heating cycles in the DSC analysis give a complete consistency. This demonstrates the reversibility of the dissociation and generation process of the adduct crystals and the repeatability of the experimental data. The data from one typical cycle of NDA-DMAC and NDA-NMP adducts are scattered in Figures 3 and 4, respectively. As can be seen for the NDA-DMAC adductive crystal, the initial dissociation temperature (T_i) is 306.29 K, and the peak temperature (T_p) is 316.19 K. The adduct crystal NDA-NMP

dx.doi.org/10.1021/je2009973 | J. Chem. Eng.Data 2012, 57, 406−411

Table 2. Main Crystal Structure Data of NDA-DMAC and NDA-NMP Adduct Crystals

	NDA-DMAC	NDA-NMP
chemical formula	$C_{20}H_{26}N_2O_6$	$C_{22}H_{26}N_2O_6$
chemical formula weight	390.43	414.45
symmetry cell setting	monoclinic	orthorhombic
symmetry space group name	*P*21/*n*	*Fdd*2
cell length *a*/Å	11.1940(6)	19.7306(11)
cell length *b*/Å	7.8328(4)	28.7632(19)
cell length *c*/Å	11.2852(6)	7.1906(4)
cell angle α/deg	90.00	90.00
cell angle β/deg	97.921(5)	90.00
cell angle γ/deg	90.00	90.00
cell volume/Å^3	980.05(9)	4080.8(4)
cell formula units *Z*	2	8
experimental crystal density/mg·m^{-3}	1.323	1.349
experimental absorpt coefficient μ/mm^{-1}	0.098	0.099
experimental crystal *F*(000)	416	1760
cell measurement temperature/K	120(2)	120(2)
diffraction reflections θ	2.7546 to 29.2788	3.0911 to 29.1661
diffraction reflections limit *h*	−13 to 11	−23 to 19
diffraction reflections limit *k*	−7 to 9	−22 to 34
diffraction reflections limit *l*	−12 to 13	−8 to 7
refinement goodness of fit on F^2	1.066	1.050
refinement *R* factor	0.0658	0.0368
refinement *wR* factor	0.1807	0.0865

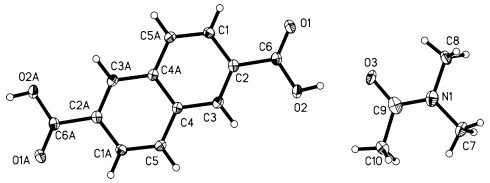

Figure 1. Molecular structure of the NDA-DMAC adduct crystal.

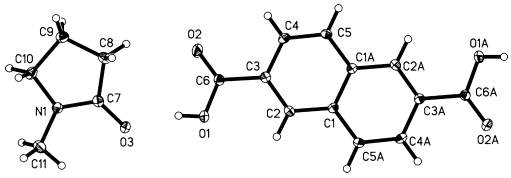

Figure 2. Molecular structure of the NDA-NMP adduct crystal.

begins to dissociate at 322.75 K and reaches the maximum at 328.19 K. The results show the poor thermal stabilities of the two adduct crystals, and the NDA-NMP adduct is relatively more stable. Increasing the temperature higher than the dissociation temperature, the adduct crystals will decompose to the pure NDA solid and the solvent. After filtering and evaporating the residual solvent, highly purified NDA can be obtained.

During the experiment, we also observed that when the adduct crystal was separated from the solvent, it would weather quickly. In this way, the highly pure NDA can be obtained from the adduct crystal, too.

The DSC analysis results also indicate that the dissociation processes of the two adduct crystals are both endothermic. The crystallization heat of NDA-DMAC adduct (H_{ac}) is about 43.95 J·g^{-1} and for NDA-NMP adduct, it is about 58.46 J·g^{-1}.

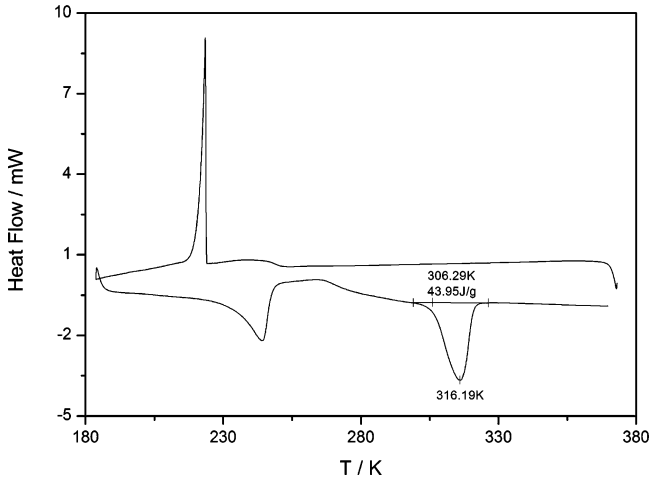

Figure 3. DSC analysis of the NDA-DMAC adduct crystal.

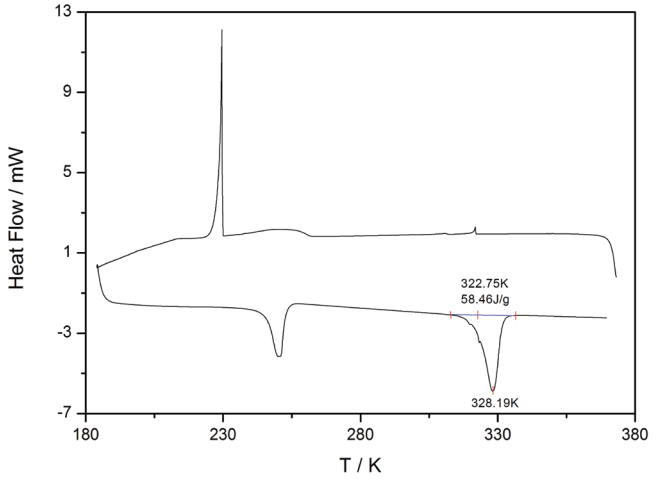

Figure 4. DSC analysis of the NDA-NMP adduct crystal.

All of the thermodynamic property data are summarized in Table 3.

Table 3. Thermodynamic Properties of NDA-DMAC and NDA-NMP Adduct Crystals

thermodynamic parameters	NDA-DMAC	NDA-NMP
T_i/K	306.29	322.75
T_p/K	316.19	328.19
H_{ac}/J·g^{-1}	43.95	58.46

Determination of the Dissolution Equilibrium Time. The experiment measuring solubility was carried out at 293.2 K first to determine the requisite time for the dissolution equilibrium. In this section, continuous stirring without any standing time was adopted to verify the sufficient blend and dissolution. Thus, to get the clear saturated NDA solution sample, a filter was installed at the head of the sampling syringe. Because the environmental temperature was quite close to 293.2 K and the sampling process was conducted as fast as possible, the deviation brought by the temperature difference between the solution and the sampling tools could be tolerant. The first sample was taken after 5 h, and then we sampled every 5 h.

dx.doi.org/10.1021/je2009973 | J. Chem. Eng.Data 2012, 57, 406−411

The experimentally determined time evolutions of NDA mole fraction in DMAC and NMP solvents are plotted in Figure 5. The mole fractions of NDA in the two solvents both

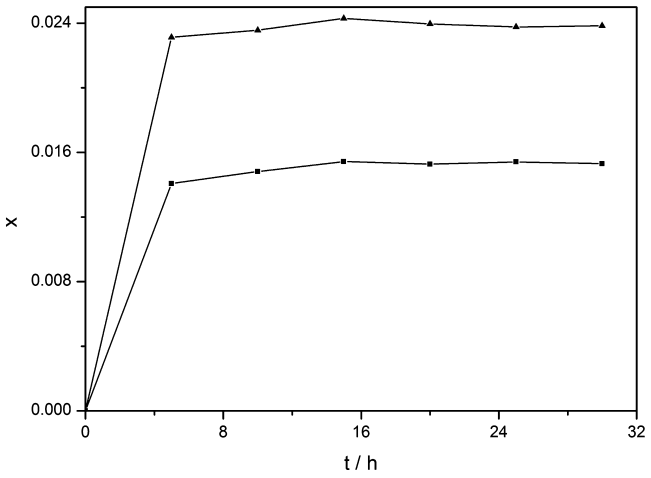

Figure 5. Mole fraction of NDA in DMAC and NMP at different sampling times at 293.2 K: ■, NDA in DMAC; ▲, NDA in NMP.

increase with time and reach a plateau after about 20 h. The equilibrium was verified by the solution composition reproducible within ± 1 %.

With the experimental temperature rising up, the dissolution equilibrium would be achieved more easily and quickly, so 20 h was also enough for the achievement of equilibrium at the temperature higher than 293.2 K. In this work, the stirring time was chosen as 24 h.

Solubilities of NDA in DMAC and NMP Solvents. The solubility of NDA in the solvent is expressed as:

$$x = \frac{n_{\mathrm{NDA}}}{n_{\mathrm{NDA}} + n_{\mathrm{sol}}} \quad (1)$$

where x stands for the mole fraction solubility of the solute NDA in the saturated solution; n_{NDA} and n_{sol} are respectively the molar concentrations of NDA and the solvent in the saturated solution.

The experimental results are listed in Tables 4 and 5 and scattered in Figures 6 and 7. As a general trend, the solubilities of NDA in DMAC and NMP solvents both increase as the experimental temperature increases.

Furthermore, it is obvious that the solubility of NDA in NMP at 323.2 K is different from the solubility evolution trends below 323.2 K or above 323.2 K. This abnormal appearance could be attributable to the thermal stability of NDA-NMP adducts. At the temperature lower than the dissociation temperature (about 322.75 K for NDA-NMP adduct), the equilibrium solid phase is NDA-NMP adduct, but when higher than it, the equilibrium solid phase is NDA solid with the adduct crystal dissociating. All that is in agreement with the theoretical phase diagram of two-component system with an unstable compound produced. Then considering the data at 323.2 K, it is quite approximate to the initial dissociation temperature of the NDA-NMP adduct crystal. It is reasonable to speculate that the equilibrium time is longer than 24 h at this temperature. So the solid phase is still unstable ,and the composition of it is uncertain within the experimental time. Therefore, the solubility data of NDA in NMP will be

Table 4. Solubility of NDA in DMAC at Temperatures Ranging from (293.2 to 373.2) K

T/K	x_{exp}	x_{cal}	RD/%
293.2	0.01536	0.01542	0.3906
298.2	0.01619	0.01620	0.0618
303.2	0.01695	0.01701	0.3540
308.2	0.01775	0.01783	0.4507
313.2	0.01879	0.01868	−0.5854
318.2	0.01973	0.01955	−0.9123
323.2	0.02046	0.02043	−0.1466
328.2	0.02132	0.02135	0.1407
333.2	0.02221	0.02228	0.3152
338.2	0.02350	0.02323	−1.1489
343.2	0.02425	0.02421	−0.1649
348.2	0.02506	0.02521	0.5986
353.2	0.02608	0.02624	0.6135
358.2	0.02741	0.02729	−0.4378
363.2	0.02827	0.02836	0.3184
368.2	0.02964	0.02946	−0.6073
373.2	0.03038	0.03059	0.6912

Table 5. Solubility of NDA in NMP at Temperatures Ranging from (293.2 to 373.2) K

T/K	x_{exp}	x_{cal}	RD/%
293.2	0.02381	0.02399	0.7560
298.2	0.02475	0.02480	0.2020
303.2	0.02595	0.02576	−0.7322
308.2	0.02715	0.02687	−1.0313
313.2	0.02820	0.02813	−0.2482
318.2	0.02924	0.02955	1.0602
323.2	0.02888	0.02985	
328.2	0.03007	0.03022	0.4988
333.2	0.03062	0.03054	−0.2613
338.2	0.03112	0.03095	−0.5463
343.2	0.03137	0.03144	0.2231
348.2	0.03216	0.03202	−0.4353
353.2	0.03269	0.03269	0.0000
358.2	0.03323	0.03344	0.6320
363.2	0.03421	0.03429	0.2338
368.2	0.03532	0.03523	−0.2548
373.2	0.03631	0.03626	−0.1377

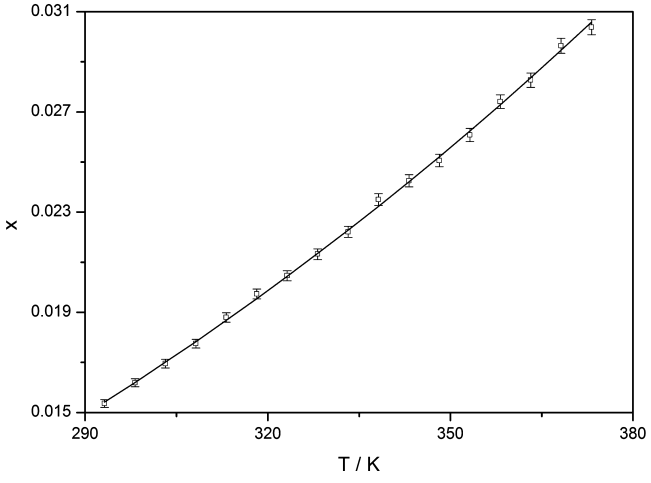

Figure 6. Solubility of NDA in DMAC: □, experimental data; line, model correlated data.

dx.doi.org/10.1021/je2009973 | J. Chem. Eng.Data 2012, 57, 406−411

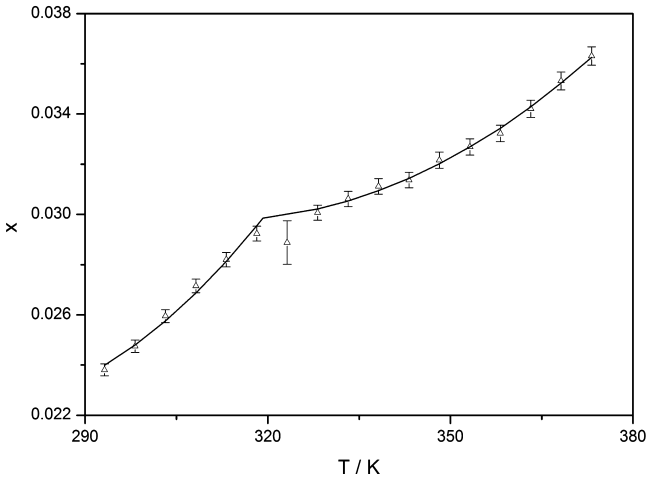

Figure 7. Solubility of NDA in NMP: △, experimental data; line, model correlated data.

correlated in low and high temperature ranges separately with the data at 323.2 K rejected.

However, for the solubility data of NDA in DMAC, the different trends in low and high temperature ranges are not obvious. This is probably due to the property of the system. In addition, the experimental temperatures here are mainly above the dissociation temperature range of the NDA-DMAC adduct except only three points, which have little influence on the general trend. So the solubility data in this system will be correlated continuously.

Correlation of Solubility Data. *Correlation with the Buchowski Equation.* The Buchowski equation, eq 2, was published by Buchowski and co-workers in 1980. This equation can be applied to most solid−liquid equilibrium systems. Although it only involves two parameters, λ and h, the model can correlate the experimental data quite well, needless to consider the activity coefficients of the components. The two parameters are almost constant as functions of temperature. λ is related to the effect of the activity of the component, and h is the enthalpic factor.[15]

$$\ln\left(1 + \frac{\lambda(1-x)}{x}\right) = \lambda h\left(\frac{1}{T} - \frac{1}{T_{\mathrm{fus,NDA}}}\right) \tag{2}$$

In eq 2, T is the absolute temperature of the solid−liquid equilibrium; $T_{\mathrm{fus,NDA}}$ is the fusion temperature of NDA, which was chosen to be 845.33 K[16] here.

The parameters, λ and h, are regressed from the experimental data by a nonlinear optimization, minimizing the difference between the correlated and experimental solubility. The objective function, F, is defined as follows:

$$F = \frac{1}{n}\sum_{i}^{n}\left((x_{\mathrm{cal},i} - x_{\mathrm{exp},i})/x_{\mathrm{exp},i}\right)^2 \tag{3}$$

where $x_{\mathrm{cal},i}$ and $x_{\mathrm{exp},i}$ are respectively the calculated and the experimental mole fraction of NDA in the saturated solution; n is the number of experimental data. Here, the simulation program was written in Matlab to achieve the optimization.

The solubility data of NDA in DMAC can be correlated by the Buchowski equation quite well. The regressed values of λ and h are listed in Table 6, and the calculated solubility data are presented in Table 4. It can be seen that the simulated values

Table 6. Model Parameters in eq 2 and NRTL Activity Coefficient Model

	model parameters				
solvent	λ			h	
DMAC	0.05653			12134.9	
	g_{11}	g_{12}	g_{21}	g_{22}	k_{NDA}
NMP (at high temperatures)	13728.7	−1805.2	−1805.2	10799.2	125.2
		$T_{\mathrm{fus,NDA-NMP}}$/K		$k_{\mathrm{NDA-NMP}}$	
NMP (at low temperatures)		578.4		251.2	

have a satisfied agreement with the experimental data, and the average relative standard deviation (ARD) of them is about 0.47 %. The ARD is defined as

$$\mathrm{ARD} = \frac{1}{n}\sum_{i=1}^{n}\mathrm{abs}\left(\frac{x_{\mathrm{cal},i} - x_{\mathrm{exp},i}}{x_{\mathrm{exp},i}}\right) \tag{4}$$

However, the Buchowski equation seems not suitable to correlate the solubility of NDA in NMP. At high temperatures of (328.2 to 373.2) K, the regressed parameter λ is negative, which is unreasonable, while at low temperatures of (293.2 to 318.2) K, the objective function cannot get a convergence. Therefore, another model is introduced.

Correlation with the NRTL Activity Coefficient Model. At a constant temperature and pressure, the solid−liquid phase equilibrium is reached when the component fugacity of NDA in the equilibrium liquid phase is equal to the one in the equilibrium solid phase:

$$\hat{f}^{\mathrm{L}}_{\mathrm{NDA}} = \hat{f}^{\mathrm{S}}_{\mathrm{NDA}} \tag{5}$$

Considering the relationship among the fugacity, activity, and activity coefficient, eq 5 becomes

$$f^{\mathrm{L}}_{\mathrm{NDA}} x^{\mathrm{L}}_{\mathrm{NDA}} \gamma^{\mathrm{L}}_{\mathrm{NDA}} = f^{\mathrm{S}}_{\mathrm{NDA}} x^{\mathrm{S}}_{\mathrm{NDA}} \gamma^{\mathrm{S}}_{\mathrm{NDA}} \tag{6}$$

where $f^{\mathrm{L}}_{\mathrm{NDA}}$ is the fugacity of pure NDA liquid; $f^{\mathrm{S}}_{\mathrm{NDA}}$ is the fugacity of pure NDA solid; $x^{\mathrm{L}}_{\mathrm{NDA}}$ and $\gamma^{\mathrm{L}}_{\mathrm{NDA}}$ are the mole fraction and the activity coefficient of NDA in the equilibrium liquid phase; $x^{\mathrm{S}}_{\mathrm{NDA}}$ and $\gamma^{\mathrm{S}}_{\mathrm{NDA}}$ are the mole fraction and the activity coefficient of NDA in the equilibrium solid phase. In this work, $x^{\mathrm{L}}_{\mathrm{NDA}}$ is just the mole fraction solubility of NDA we have measured.

Combining eq 6 and the relationship between $f^{\mathrm{L}}_{\mathrm{NDA}}$ and $f^{\mathrm{S}}_{\mathrm{NDA}}$ (assuming a pure solid phase), we get

$$x^{\mathrm{L}}_{\mathrm{NDA}} \gamma^{\mathrm{L}}_{\mathrm{NDA}} = \exp\left(\frac{\Delta_{\mathrm{fus}} h_{\mathrm{NDA}}}{R}\left(\frac{1}{T_{\mathrm{fus,NDA}}} - \frac{1}{T}\right)\right) \tag{7}$$

where $\Delta_{\mathrm{fus}} h_{\mathrm{NDA}}$ is the molar enthalpy of fusion for NDA; R is the universal gas constant, which was 8.314 J·mol^{-1}·K^{-1} here.

Unfortunately, the value of $\Delta_{\mathrm{fus}} h_{\mathrm{NDA}}$ is unknown. We used the following empirical equation[17] to estimate it.

$$\Delta_{\mathrm{fus}} h_{\mathrm{NDA}} = k_{\mathrm{NDA}} T_{\mathrm{fus,NDA}} \tag{8}$$

where k_{NDA} is an empirical parameter regressed from the experimental data.

To calculate the activity coefficients, the nonrandom two-liquid (NRTL) activity coefficient model[18] which is expressed by eq 9 was adopted here.

dx.doi.org/10.1021/je2009973 | J. Chem. Eng.Data 2012, 57, 406−411

$$\ln \gamma_1 = x_2^2\left[\frac{\tau_{21}G_{21}{}^2}{(x_1 + x_2G_{21})^2} + \frac{\tau_{12}G_{12}}{(x_2 + x_1G_{12})^2}\right] \quad (9)$$

where γ_i and x_i are the activity coefficient and the mole fraction of component i; τ_{ij} and G_{ij} are parameters calculated by

$$\tau_{ij} = \frac{g_{ij} - g_{jj}}{RT} \qquad G_{ij} = \exp(-\alpha_{ij}\tau_{ij})$$
$$g_{ij} = g_{ji} \qquad \alpha_{ij} = \alpha_{ji} \qquad \alpha_{ii} = 0 \quad (10)$$

where g_{ij} and α_{ij} are parameters to be optimized.

In eq 9, the subscript 1 stood for NDA, and 2 stood for NMP. In eq 10, the parameter, α_{ij}, was chosen as 0.3, which was proposed by Renon and Prausnitz.[19]

The equations and derivations above can be found in a common textbook about solid−liquid equilibrium, such as Prausnitz et al.[20]

First the solubility data of NDA in NMP solvent at high temperatures of (328.2 to 373.2) K were correlated by the model above. The equilibrium solid phase was NDA solid. The optimization objective function was eq 3. The parameters g_{ij} and k_{NDA} were taken to be optimized.

Then the solubility data of NDA in NMP solvent in the low temperature range were correlated in the same way, while the equilibrium solid phase was NDA−NMP adduct and the solubility was expressed in the form of NDA−NMP adduct instead of NDA during the optimization. The melting point of NDA−NMP adduct, $T_{fus,NDA-NMP}$, was added to the optimized parameters. To be emphasized, there was an approximation here that the parameter g_{ij}, which represented the interaction among the molecules in the liquid phase, in these two temperature ranges were treated as the same because the two systems had no essential difference in the liquid phase.

The optimized model parameters are listed in Table 6 and the calculated solubility values, which have a great consistency with the experimental data with the ARD only about 0.45 %, are given in Table 5.

All of the correlated solubilities are plotted in Figures 6 and 7 for comparison with the experimental solubilities.

AUTHOR INFORMATION

Corresponding Author

*E-mail: ywcheng@zju.edu.cn.

Funding

We express cordial acknowledgment for the financial support from the National Science Foundation of China (No. 20806072) and the Research Fund for the Doctoral Program of Higher Education of China (No. 200803351111).

REFERENCES

(1) Gao, X.; Liu, R.; Zhang, J.; Zhang, J. Crystallization Behaviors of Poly(ethylene 2,6-naphthalate) in the Presence of Liquid Crystalline Polymer. *Ind. Eng. Chem. Res.* **2008**, *47*, 2590−2596.

(2) Lillwitz, L. D. Production of dimethyl-2,6-naphthalenedicarboxylate: precursor to polyethylene naphthalate. *Appl. Catal. A: Gen.* **2001**, *221*, 337−358.

(3) Martin, A.; Armbruster, U.; Muller, P.; Deuschle, E. Oxidative conversion of alkyl naphthalenes to carboxylic acids in hot pressurised water. *J. Supercrit. Fluids* **2008**, *45*, 220−224.

(4) Harper, J. J.; Kuhlmann, G. E.; Larson, K. D.; McMahon, R. F.; Sanchez, P. A. Process for preparing 2,6-naphthalene-dicarboxylic acid. U.S. Patent US5183933, 1993.

(5) Albertins, R.; Pietsch, S. J.; Holzhauer, J. K.; Schroeder, H. Method for purifying a crude naphthalene dicarboxylic acid. U.S. Patent US4933491, 1990.

(6) Iwane, H.; Sugawara, T.; Shirasaki, M. Process for purification of naphthalenedicarboxylic acid. U.S. Patent US5344969, 1994.

(7) Holzhauer, J. K.; Young, D. A. Process for Preparing Purified Dimethyl Naphthalenedicarboxylate. U.S. Patent US5254719, 1993.

(8) Cheng, Y.; Wu, B.; Li, X.; Wang, L.; Zheng, K. Process for preparing high purity 2,6-naphthalene-dicarboxylic acid. China Patent CN 102070442 A, 2011.

(9) Schoen, H. M.; Mcketta, J. J. *New chemical engineering separation techniques*; Interscience Publishers: New York, 1962.

(10) Cheng, Y.; Peng, G.; Wu, B.; Guo, X.; Li, X. Thermodynamic Study on the Adduct Crystallization of Terephthalic Acid with Amides. *J. Chem. Eng. Data* **2011**, *56*, 1020−1024.

(11) Wu, B.; Peng, G.; Cheng, Y.; Li, X.; Liu, J. Naphthalene-2,6-dicarboxylic acid−1-methylpyrrolidin-2-one (1/2). *Acta Crystallogr., Sect. E* **2011**, *67*, o208.

(12) Guo, X.; Cheng, Y.; Wang, L.; Li, X. Solubility of Terephthalic Acid in Aqueous N-Methyl Pyrrolidone and N,N-Dimethyl Acetamide Solvents at (303.2 to 363.2) K. *J. Chem. Eng. Data* **2008**, *53*, 1421−1423.

(13) Oxford Diffraction. *CrysAlis PRO*; Oxford Diffraction Ltd.: Yarnton, England, 2009.

(14) Sheldrick, G. M. A Short History of SHELX. *Acta Crystallogr., Sect. A* **2008**, *64*, 112−122.

(15) Buchowski, H.; Ksiazczak, A.; Pietrzyk, S. Solvent Activity along a Saturation Line and Solubility of Hydrogen-Bonding Solids. *J. Phys. Chem.* **1980**, *84*, 975−979.

(16) Ma, P.; Xia, Q. Determination and Correlation for Solubility of Aromatic Acids in Solvents. *Chin. J. Chem. Eng.* **2001**, *9*, 39−44.

(17) Tong, J.; Li, J. *Calculation of Fluid Thermophysic Properties*; Qinghua University Press: Beijing, 1982.

(18) Renon, H.; Prausnitz, J. M. Local Compositions in Thermodynamic Excess Functions for Liquid Mixtures. *AIChE J.* **1968**, *14*, 135−144.

(19) Renon, H.; Prausnitz, J. M. Estimation of Parameters for NRTL Equation for Excess Gibbs Energy of Strongly Nonideal Liquid Mixtures. *Ind. Eng. Chem., Process Des. Dev.* **1969**, *8*, 413−419.

(20) Prausnitz, J. M.; Lichtenthaler, R. N.; De Azevedo, E. G. *Molecular Thermodynamics of Fluid-Phase Equilibria*; Prentice Hall: Englewood Cliffs, NJ, 1999.